Letters in High Energy Physics
ISSN: 2632-2714
Volume 2024

Comparison between CP-Ti and Ti 6Al 4V alloys in terms of weight loss using the Tribocorrosion Test.

Taha Obayes Mohammed Al-Kelabi [1'a]) and Zuheir Talib Khulief [2'b])

[1'2]) Metallurgical Engineering, Materials Engineering College, University of Babylon, Iraq

[a]) talkelabi@jmail.com

[b]) mat.zuheir.talib@uobabylon.edu.iq

Abstract. This paper is concerned with studying the tribocorrosion of CP-Ti and Ti 6Al 4V alloys used for biomedical applications and compare the results and then choose the best alloy. This research is divided into two parts. The first part is to characterize the alloys using XRD, OM, SEM, and XRF. The second part includes making a tribocorrosion test for the alloys (cathodic potential, anodic potential, and open circuit potential) using three different loads (1N ,2N and 4N). calculating the coefficient of friction and the effect of the load applied to it, as well as calculating the lost weight resulting from the mechanical effect and the electrochemical effect during the test . Metal characterization methods (SEM, XRD,XRF and OM) showed that CP-Ti consisted of single phases (α) as expected and Ti 6Al 4V consisted of two phases α + β as expected (α -rich). The test showed that load has an effect on the coefficient of friction, as the coefficient increases with increasing load and as a result an increase in the lost weight.

Keywords: tribocorrosion, CP-Ti, Ti 6Al 4V, biomedical

INTRODUCTION

The Titanium and Titanium alloys are widely utilized in biomedical fields as implant materials because of their excellent resistance of corrosion, low density, high biocompatibility and high specific strength as compared to other materials which used in biomedical field such as St.St and Co-based alloys [1,2]. In spite of the Titanium and its alloy doesn't cause any toxicity during service due to its good biocompatibility, its mechanical properties unadequite for some applications where high strength is needed such as hard tissue replacements or intensive wear applications [1,2].

The performance of corrosion of Titanium alloys inspected in aqueous sol by Kelly et al. [3]. They decided that there are four reactions [3]. The first one is the active reaction , Titanium can be oxidized with a high oxidation rate creating Ti (III) ions. The second is the passive reaction , in which the oxidation rate is reduced greatly because of that titanium is covered by stable and protective oxide layers. By increasing the immersion time, Ti (IV) ions can be formed , this ion could migrate throw the oxide layer or enter the solution. The third reaction is the active-passive state, also known as the translational state. In this state, the oxide film partially covers the titanium surface, which hinders the full passivation of the titanium. The fourth reaction is the hydrogen evolution state, where titanium can undergo corrosion due to hydrogen evolution when subjected to a sufficiently negative potential [3]. Therefore, the reactions are influenced by multiple environmental factors, including exposure time, temperature, and pH..[3].

Some elements like Nb, Mo, Ta, and Zr, when added to titanium, stabilize the oxide layer on the surface under physiological conditions due to the formation of oxides of these elements [4,5].

Single-phase titanium alloy(α or β phase) is more resistant to corrosion than two-phase titanium alloy

(α + β or β +α phase) [6] .

EXPERIMENTAL

In this study, CP-Ti and Ti 6Al 4V alloys were used. Before testing, the alloys were cut from a rod into disc pieces measuring 15mm in diameter and 3mm in thickness using a wire cutter. Both surfaces of the samples were then ground with SiC papers ranging from 800 to 3000 grit size. Subsequently, the samples were polished with a 0.1-micron grain size diamond paste. After polishing, the samples were etched according to ASTM E407-07, washed with distilled water, and finally cleaned with ethanol in an ultrasonic bath . The microstructures of the alloys were analyzed using optical microscopy

(OM), X-ray diffraction (XRD), scanning electron microscopy (SEM), and X-ray fluorescence (XRF). The phases present were identified using XRD analysis at room temperature. The microstructures were examined with optical microscopy, and SEM was used to analyze the distribution of phases and elements within the alloy. Additionally, the percentages of elements in the alloys were determined using XRF. The tribocorrosion test of the alloys were carried out using OCP, cathodic potential and anodic potential under the effect of three different loads (1,2 and 4 N) in Phosphate Buffered Saline (PBS). The chemical composition of the (PBS) is consisting of phosphate buffer saline with the addition of 15 g/L of Bovine Serum Albumin[7]. The test was applied to the samples for an hour at a frequency of 5 Hz and with a movement distance of 6 mm for all three tests above, and a sliding distance of 217m was achieved. The instantaneous coefficient of friction, current and voltage were calculated after every second of time. The wear volume for each test was measured by measuring the width of the wear track according to Equations 1 , 2 and 3 [8,9].

$$\mathbf{Vt = A.L} \qquad \mathbf{(1)}$$

Where Vt is total volume of the material loss

L = 6mm (stroke length) and

A= wear track cross section area

$$\boldsymbol{A = \frac{R^2(\theta - sin\theta)}{2}} \qquad \mathbf{(2)}$$

R = 2.5 mm(ball radius and

θ is the angle of the circular segment which forms the wear track

$$\boldsymbol{\theta = 2\sin^{-1}(\frac{a}{2R})} \qquad \mathbf{(3)}$$

a is the width of wear track.

RESULTS AND DISCUSSION

The OM images of CP-Ti and Ti 6Al 4V are shown in Figure 1. The SEM images of CP-Ti and Ti 6Al 4V are shown in Figure 2. The microstructure of CP-Ti was single phase (α phase). The microstructure of Ti 6Al 4V consisted of two phases α + β as expected (α -rich). This fact is demonstrated by the XRD result shown in Figures 3 and 4 . The percentage of presence elements were demonstrated by the XRF examination result shown in Figures 5 and 6 .

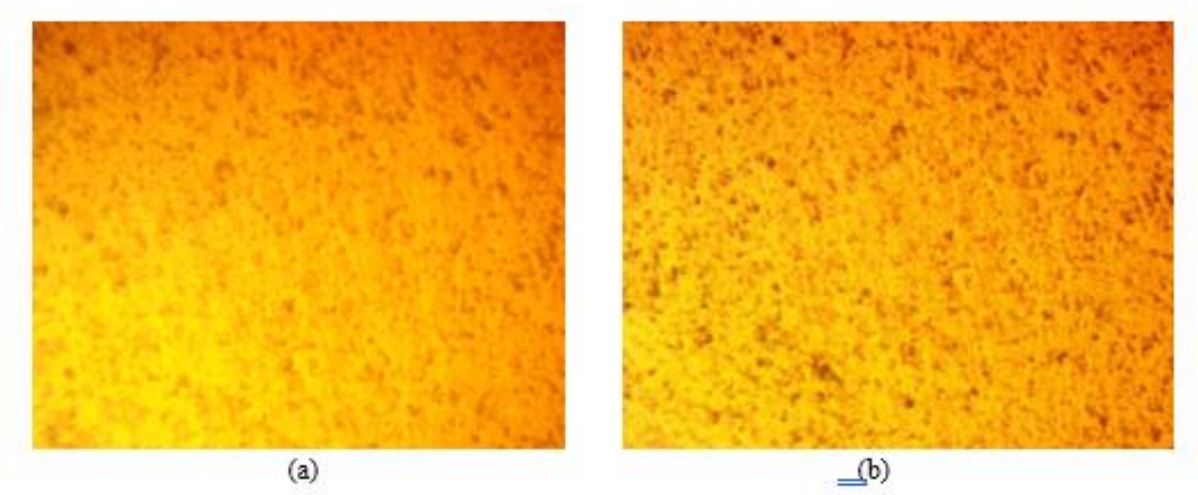

FIGURE1. OM images for (a) CP-Ti and (b) Ti 6Al 4V

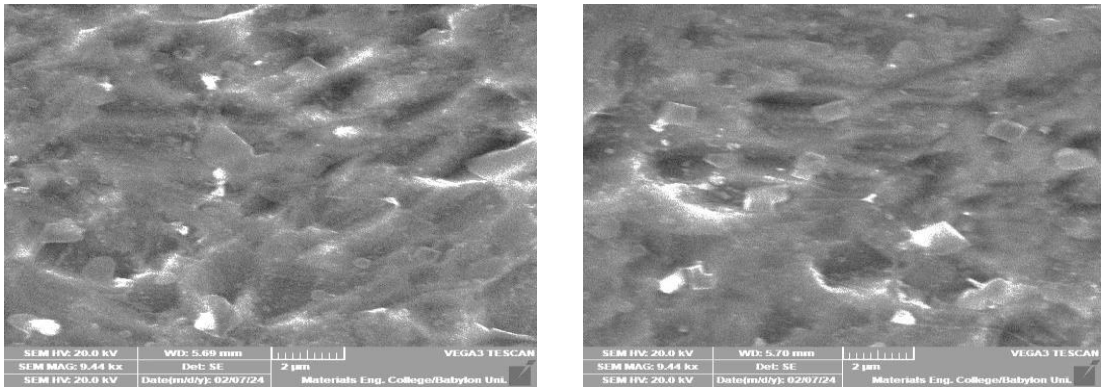

(a) (b)

FIGURE2. SEM images for (a) CP-Ti and (b) Ti 6Al 4V

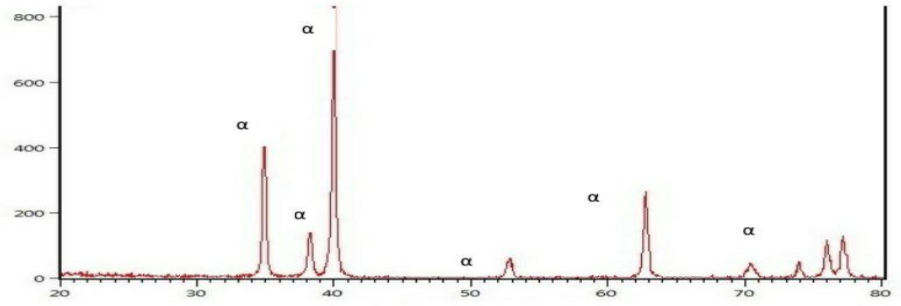

FIGURE3. XRD examination for CP-Ti alloy.

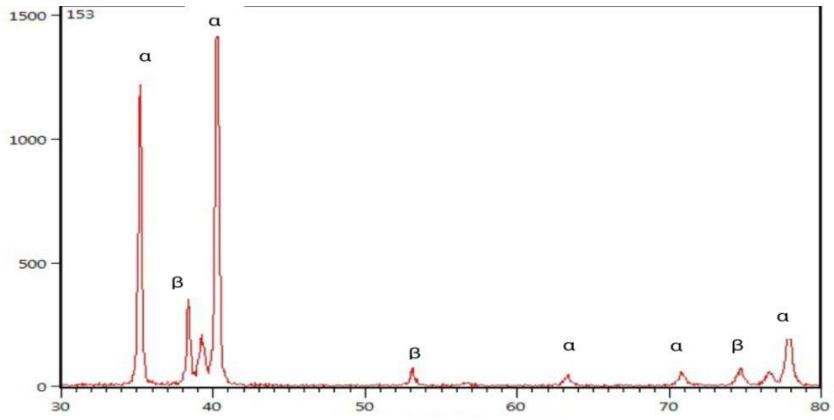

FIGURE4. XRD examination for Ti 6Al 4V alloy.

Z	Symbol	Element	Concentration		Abs. Error	
12	Mg	Magnesium	< 0.034	%	(0.0)	%
13	Al	Aluminum	< 0.0074	%	(0.0)	%
14	Si	Silicon	< 0.0025	%	(0.0)	%
15	P	Phosphorus	< 0.0015	%	(0.0)	%
16	S	Sulfur	< 0.0020	%	(0.0)	%
22	Ti	Titanium	98.33	%	0.13	%
23	V	Vanadium	< 0.051	%	(0.0)	%
24	Cr	Chromium	0.0129	%	0.0022	%
25	Mn	Manganese	0.0129	%	0.0055	%
26	Fe	Iron	0.3284	%	0.0089	%
27	Co	Cobalt	0.0083	%	0.0033	%
28	Ni	Nickel	0.0977	%	0.0037	%
29	Cu	Copper	0.0165	%	0.0027	%
30	Zn	Zinc	0.0825	%	0.0024	%
33	As	Arsenic	0.00214	%	0.00029	%
40	Zr	Zirconium	< 0.0100	%	(0.0)	%
41	Nb	Niobium	0.0098	%	0.0027	%
42	Mo	Molybdenum	0.0857	%	0.0073	%
47	Ag	Silver	0.0021	%	0.0014	%
48	Cd	Cadmium	0.00177	%	0.00090	%
50	Sn	Tin	< 0.0016	%	(0.0)	%
51	Sb	Antimony	< 0.0011	%	(0.0)	%
74	W	Tungsten	0.0053	%	0.0035	%
82	Pb	Lead	< 0.00081	%	(0.0)	%
Sum of concentration			99.00	%		

FIGURE5. XRF examination for CP-Ti alloy.

Z	Symbol	Element	Concentration		Abs. Error	
12	Mg	Magnesium	< 0.031	%	(0.0)	%
13	Al	Aluminum	0.0985	%	0.0052	%
14	Si	Silicon	< 0.0024	%	(0.0)	%
15	P	Phosphorus	< 0.0013	%	(0.0)	%
16	S	Sulfur	< 0.0020	%	(0.0)	%
22	Ti	Titanium	92.92	%	0.13	%
23	V	Vanadium	> 5.154	%	0.072	%
24	Cr	Chromium	< 0.020	%	(0.0)	%
25	Mn	Manganese	0.0129	%	0.0064	%
26	Fe	Iron	0.508	%	0.012	%
27	Co	Cobalt	< 0.0028	%	(0.0)	%
28	Ni	Nickel	0.0805	%	0.0038	%
29	Cu	Copper	0.0087	%	0.0029	%
30	Zn	Zinc	0.0901	%	0.0028	%
33	As	Arsenic	0.00172	%	0.00033	%
40	Zr	Zirconium	< 0.012	%	(0.0)	%
41	Nb	Niobium	0.0107	%	0.0032	%
42	Mo	Molybdenum	0.1092	%	0.0083	%
47	Ag	Silver	< 0.00081	%	(0.0)	%
48	Cd	Cadmium	< 0.00077	%	(0.0)	%
50	Sn	Tin	< 0.00035	%	(0.0)	%
51	Sb	Antimony	0.0010	%	0.0010	%
74	W	Tungsten	< 0.0027	%	(0.0)	%
82	Pb	Lead	< 0.00084	%	(0.0)	%

FIGURE6. XRF examination for Ti 6Al 4V alloy

TRIBOCOROSSION TEST

The average coefficient of friction for the OCP, anodic and cathodic tests under the effect of three different loads (1,2 and 4 N) is shown in Figures 7 , 8 and 9 respectively. We notice that the friction coefficient increases with the increasing applied load , and Its value is greater when a cathodic potential is applied and less when an anodic potential is applied, and the values are between the two values for the OCP test. In general, we observe that the coefficient of friction for the Ti 6Al 4V alloy is lower than that of the CP-Ti alloy.

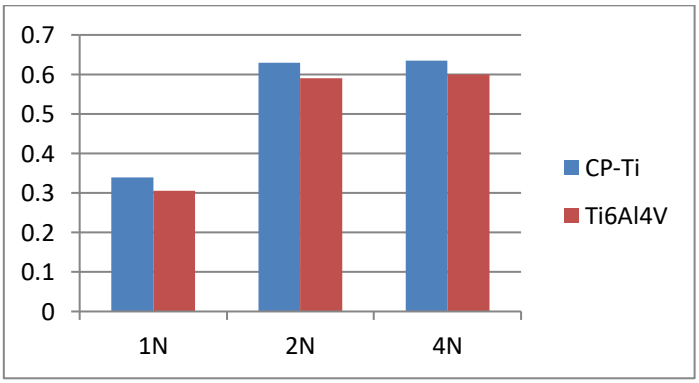

FIGURE7. The average coefficient of friction measured during the OCP test at three different loads.

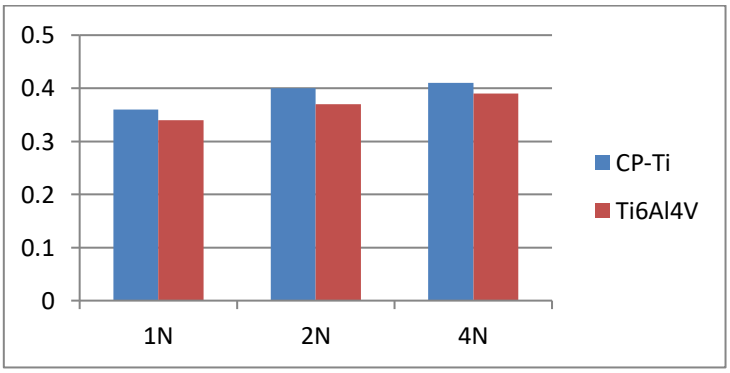

FIGURE8. The average coefficient of friction measured during applied anodic potential at three different loads.

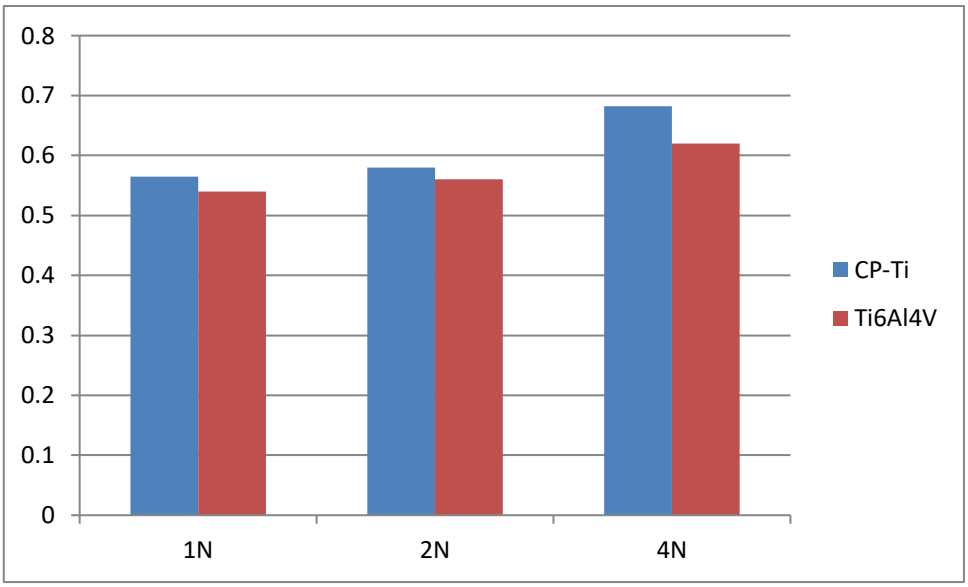

FIGURE8. The average coefficient of friction measured during applied cathodic potential at three different loads.

After conducting the tribocorrosion test under the application of a cathodic potential on the CP-Ti alloy, the wear track width was measured using SEM. The wear track width values were found to be 1376.33, 1665.16, and 1959.97 micrometers under loads of 1, 2, and 3, respectively.

For OCP test (559.92, 805.41 and 1042 µm respectively)

For anodic test (598.92 , 690.98 and 737.01 µm respectively) .
By applying equations 1,2 and 3, the wear volume values are shown in Table 1.

Table 1. Wear track volumes for cathodic, OCP and anodic tests under three different loads.

Test	Loads (N)	Wear Track Volume(mm)
Cathodic	**1**	**0.512**
	2	**0.919**
	4	**1.549**
OCP	**1**	**0.035**
	2	**0.1**
	4	**0.22**
Anodic	**1**	**0.033**
	2	**0.061**
	4	**0.075**

In the same manner, the wear track volume of the Ti 6Al 4V alloy was calculated, and the values are shown in Table 2.

Table 2. Wear track volumes for cathodic, OCP and anodic tests under three different loads.

Test	Loads (N)	Wear Track Volume(mm)
Cathodic	1	0.481
	2	0.83
	4	1.311
OCP	1	0.0331
	2	0.0896
	4	0.175
Anodic	1	0.031
	2	0.058
	4	0.061

We notice that the wear volume amount increases with the increase in the applied load. Also, the amount of wear volume is the largest value when a cathodic potential is applied, less than that in the OCP test, and the lowest value when an anodic potential is applied. As we can observe, the wear track volume in the Ti 6Al 4V alloy is generally lower than its value in the CP-Ti alloy.

CONCLUSION

The main conclusions given from the research can be drown:

1. Increasing the applied load increases the value of the coefficient of friction.

2. The value of friction coefficient is larger when cathodic potential is applied and little than that in OCP, and the lowest value is when applying anodic potential.

3. The amount of wear volume increases with the increase in the applied load.

4. The amount of wear volume is highest when a cathodic potential is applied and the lowest value when an anodic potential is applied and between the two values in the OCP test.

5. In general, the wear track volume in the Ti 6Al 4V alloy is lower than in the CP-Ti alloy, which makes this alloy more favorable for biomedical applications under the conditions studied in this research.

REFERENCES

1. M. J. Donachie, Titanium: a technical guide: ASM international, 2000.

2. M. J. Donachie, "Titanium," A Technical Guide, ASM International, Materials Park, OH, 2000.

3. R. G. Kelly, J. R. Scully, D. Shoesmith, and R. G. Buchheit, Electrochemical techniques in corrosion.

4. I. Polmear, Light alloys: from traditional alloys to nanocrystals: ButterworthHeinemann, 2005.

5. W.-F. Ho, "A comparison of tensile properties and corrosion behavior of cast Ti–7.5 Mo with cp Ti, Ti–

6. L. De Almeida, I. Bastos, I. Santos, A. Dutra, C. Nunes, and S. Gabriel, "Corrosion resistance of aged Ti–Mo–Nb alloys for biomedical applications," Journal of Alloys and Compounds, vol. 615, pp. S666- S669, 2014.

7. " Molecular Cloning: A Laboratory Manual" by Sambrook and Russell

8. Mischler, S., et al., Effect of Corrosion on the Wear Behavior of Passivating Metals in Aqueous. Thin Films in Tribology, 1993. p. 245. 248.

9. Jemmely, P., et al., Tribocorrosion behaviour of Fe–17Cr stainless steel in acid and alkaline solutions. Tribology International, 1999. 32(6): p. 295- 303.

10. Rehman, A., Shah, S. A. H., Nizamani, A. U., Ahsan, M., Baig, A. M., & Sadaqat, A. (2024). AI-Driven Predictive Maintenance for Energy Storage Systems: Enhancing Reliability and Lifespan. PowerTech Journal, 48(3). https://doi.org/10.XXXX/powertech.v48.113 :contentReference[oaicite:0]{index=0}